Development of a New Type Snow Fence with Airfoil Snow Plates to Prevent Blowing-Snow Disasters:
Part 1, Evaluation of Performance by Blowing-Snow Simulation in a Wind Tunnel

Hiroshi SAKAMOTO
Professor, Kitami Institute of Technology
Masaru MORIYA
Associate Professor, Kitami Institute of Technology
Kazunori TAKAI
Research Scientist, Kitami Institute of Technology
Yoshihiro OBATA
Research Scientist, Kitami Institute of Technology

ABSTRACT

A new snow fence with airfoil snow plates to prevent snowdrift formation and improve visibility on roadways was developed. It was designed in accordance with aerodynamic principles, and its performance evaluated in a wind tunnel test in which natural snow particles were used to simulate blowing snow. Snowdrifts and visibility blockage behind the snow fence were found to be caused by the alternating rolling-up of the bottom gap flow and shear layer separatsion from the top of the fence. Use of airfoil snow plates prevented the alternating rolling-up of the bottom gap flow and shear layer separatsion from the top of the snow fence. On the basis of this finding, airfoil snow plates of optimum configuration were designed to prevent the alternating rolling-up of the flow behind the snow fence. As compared to the conventional one, this newly developed snow fence with the airfoil snow plates performed well in preventing the formation of snowdrifts and in improving visibility.

1. INTRODUCTION

Safe travel on roadways in winter in cold regions is a very serious problem that can affect the economic activities of the regions. Primary traffic difficulties experienced on roads in winter are the deterioration of visibility and snowdrift formation caused by blowing snow (Yamada et al. 1988). In cold regions, snowdrifts and visibility blockage due to blowing snow are the most frequent causes of traffic accidents on winter roads. In recent years, with the increase in the number of vehicles on the road, blowing-snow disasters have caused traffic accidents that involve a considerable number of automobiles. Blow-off type snow fences commonly are used as a countermeasure to prevent such disasters, but the blow-off performance of the conventional snow fence is limited, the fences only being effective for a downstream distance $1.5-2.0$ times the height of the snow fence (3 m$-$3.3 m) (Sakamoto et al. 1992). On two-lane roadways with an adjacent sidewalk 2 m$-$3 m wide (road width; 13 m) or four-lane roadways (road width; 20 m), visibility blockage and snowdrifts may occur in opposite traffic-lanes beyond the center-line of the roadway. A snow fence which has high blow-off performance for a 20 m wide road therefore is strongly desired. Because the snow fence used at present was developed about thirty years ago, its shape is outdated, and snow fence performance has changed very little from thirty years ago (Ishimoto et al. 1984). Moreover, as they are based on

field observations, performance evaluations have been made only for measurements of snowdrifts around a snow fence (Takeuchi 1989, 1996). Furthermore, evaluations of visibility, which are of utmost importance have rarely been made.

The performance of blow-off type snow fences primarily depends on four snow plates installed at regular intervals. In the conventional model, because hardly any flow passes through these plates, a large-scale vortex forms behind the snow fence. As a result, the rolling-up of blowing snow occurs at a distance downstream that is $1.5-2.0$ times the snow fence height, due to the alternating rolling-up of the bottom gap flow and the shear layer being separated from the top of the snow fence, which causes visibility blockage and snowdrifts. To improve its blowing-off performance, we replaced the flat snow plates of the conventional snow fence with Joukowsky airfoil snow plates and circular arc airfoil snow plates that have a wide angle of attack. The design of these airfoil snow plates was based on aerodynamic principles, and the optimum configuration of the plates was determined in wind tunnel tests for various shapes, sizes, and set-up angles. In addition, the performance of this newly developed snow fence with airfoil snow plates was investigated in wind tunnel tests, in which natural snow particles were used to simulate blowing snow and in field investigations using a prototype snow fence model.

2. EXPERIMENTAL ARRANGEMENTS AND PROCE-DURES

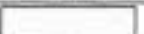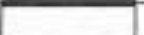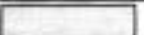### 2.1   Blowing-snow simulation in a wind tunnel

Snow fence performance can be evaluated from the blowing-off effect (prevention of snowdrifts) and density distributions of blowing snow (visibility blockage). These criteria were examined in a blowing-snow wind tunnel, in which natural snow particles were used (Sakamoto et al. 1998). The test section of the wind tunnel had a 1.3×1.3 m cross section and was 10m long. To produce blowing snow, natural snow particles were uniformly distributed over a mobile sheet on a floor to a depth of 6 cm－ 7 cm within approximately 4 m of the entrance of the test section (Fig.1). The distributed particles were blown by wind generated by four fans installed at the entrance of the wind tunnel. The blowing of the particles usually was obtained at the near upstream side of the distributed snow by slowly winding up the snow-covered mobile sheet at a velocity of 0.5 cm/s and rotating a brush installed at the near upstream end of the sheet at n=150 rpm. In addition, because the blowing of the snow particles was based on the rotational frequency of the brush, a considerable amount of blowing snow would be generated intermittently. A 1/8－1/6 model of the prototype snow fence was installed 4.8 m downstream from the entrance of the test section. The wind velocity was varied in the range of 6 m/s－8 m/s. The behavior of the blowing snow around the snow fence model was observed by irradiation with a uniform light sheet from a slit light apparatus attached to the ceiling of the test section and recorded with a CCD camera through transparent Plexiglas set in the side of the test section. Because the intensity of the light scattered from snow particles is considered to increase with the particle concentration, the light intensity distribution in the blowing-snow image recorded with the CCD camera is thought to indicate the spatial concentration distribution of the snow particles. The recorded images therefore were replaced frame by frame, the image of each frame being digitized and stored in a computer by means of a video digitizer at 256 grades per pixel for 400 pixels in the vertical and 512 pixels in the horizontal direction. The digitized images were classified into six grade ranges (Table 1), and the contour line of each range was drawn on the computer screen. The corresponding Reynolds number R_H (=UH/ν) based on the height of the snow fence model, H, in the blowing-snow wind tunnel was $(1.68-3.0)\times10^5$.

2.2   Water channel and wind tunnel experiment

Flow-visualized observations were made in a water channel in which the test section was 0.33 m deep, 0.25 m wide and 1.5 m long (Fig.2). The hydrogen bubble method was used for flow visualization. Hydrogen bubbles were generated by tungsten wire 20 μ m in diameter. A 1/22-scale model of the prototype snow fence was used, and the experiment done at the constant velocity of 6 cm/s. The corresponding Reynolds number, R_H was 6.8×10^3. In addition, velocity distributions behind the snow fence were investigated in a low-speed, closed-circuit wind tunnel (Fig.3). The test section of this wind tunnel was rectangular; height 1.2 m, width 0.3 m and length 2.5 m. The velocity distribution was measured with a yaw-type pitot tube that had four holes which allowed the direction and velocity of flow to be measured simultaneously. The free-stream velocity was constant at 10 m/s. The size of the snow fence model used was 1/10 that of the prototype snow fence. The corresponding Reynolds number, R_H, was 1.85×10^5.

Table 1.   Classification of light and shade distribution of 256 graded digital images.

Classification of light and shade intensity	Gradation range	Degree of light and shade
I	64－95	
II	96－127	
III	128－159	
IV	160－191	
V	192－223	
VI	224－255	

Fig. 1   Schematic view of the blowing-snow wind tunnel

DEVELOPMENT OF A NEW TYPE SNOW FENCE WITH AIRFOIL SNOW PLATES TO PREVENT BLOWING-SNOW DISASTERS:
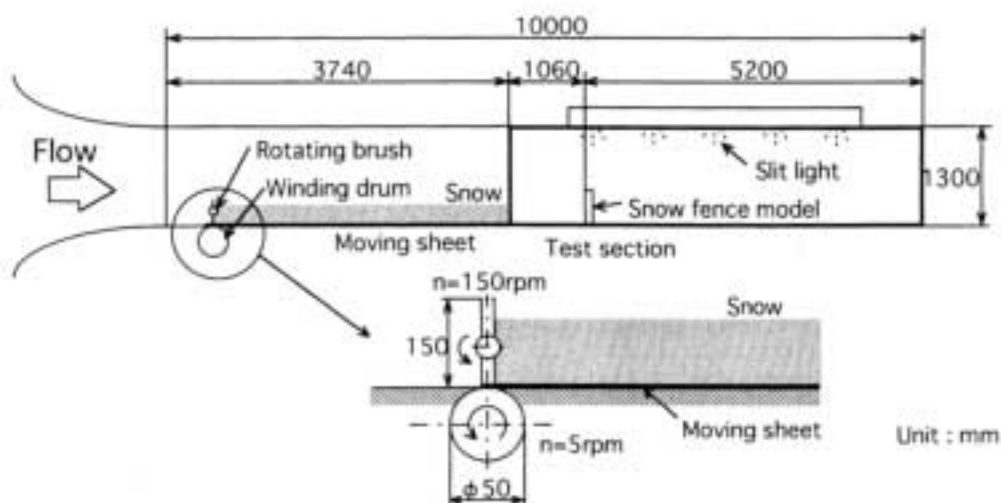*PART 1, EVALUATION OF PERFORMANCE BY BLOWING-SNOW SIMULATION IN A WIND TUNNEL*
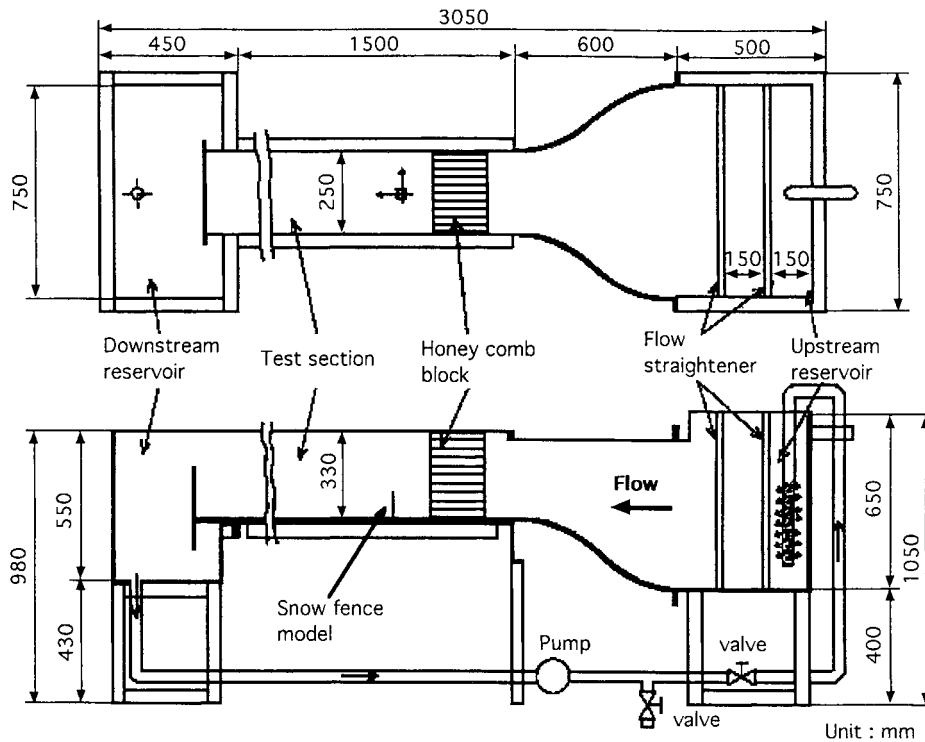
3

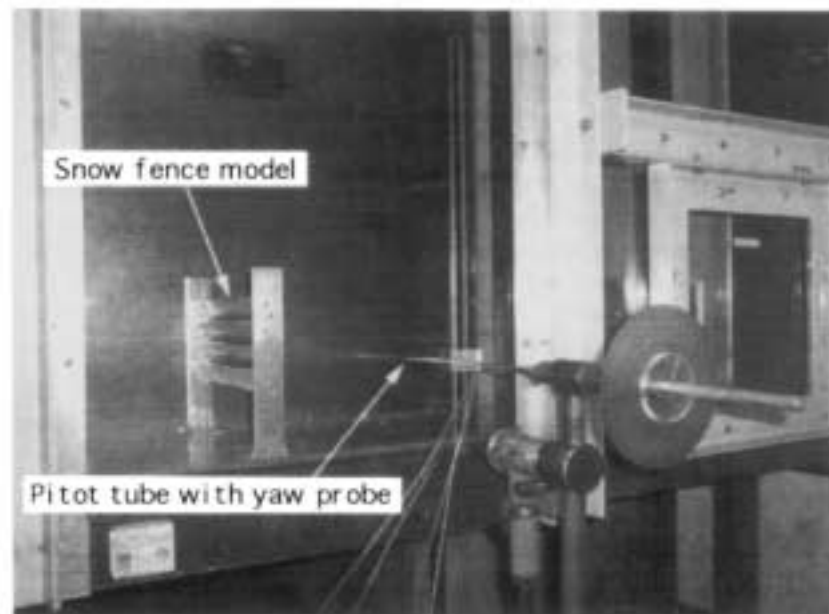Fig. 2   Water channel used for flow visualization

Fig. 3   Wind tunnel used for velocity measurements

2.3   The developed snow fence model

The models are shown in Fig.4 (a) and (b), and a conventional snow fence with a snow plate size of *W*=600 mm and setup angle of β =23.5° is shown in Fig 4(c). The newly developed snow fence has airfoil snow plates that differ completely from the flat type snow plates used in the conventional snow fence. These airfoil snow plates are of two types; a Joukowsky airfoil snow plate and a circular arc airfoil snow plate (Fig.5). Each of these airfoil snow plates consists of two subtypes (Types A and B). The circular arc airfoil snow plates differ in the shape of the circular arc of the leading edge, and the Joukowsky airfoil snow plates differ in the camber line. Furthermore, each of these airfoil snow plate types was produced in three sizes, all of which were geometrically similar (Fig.5).
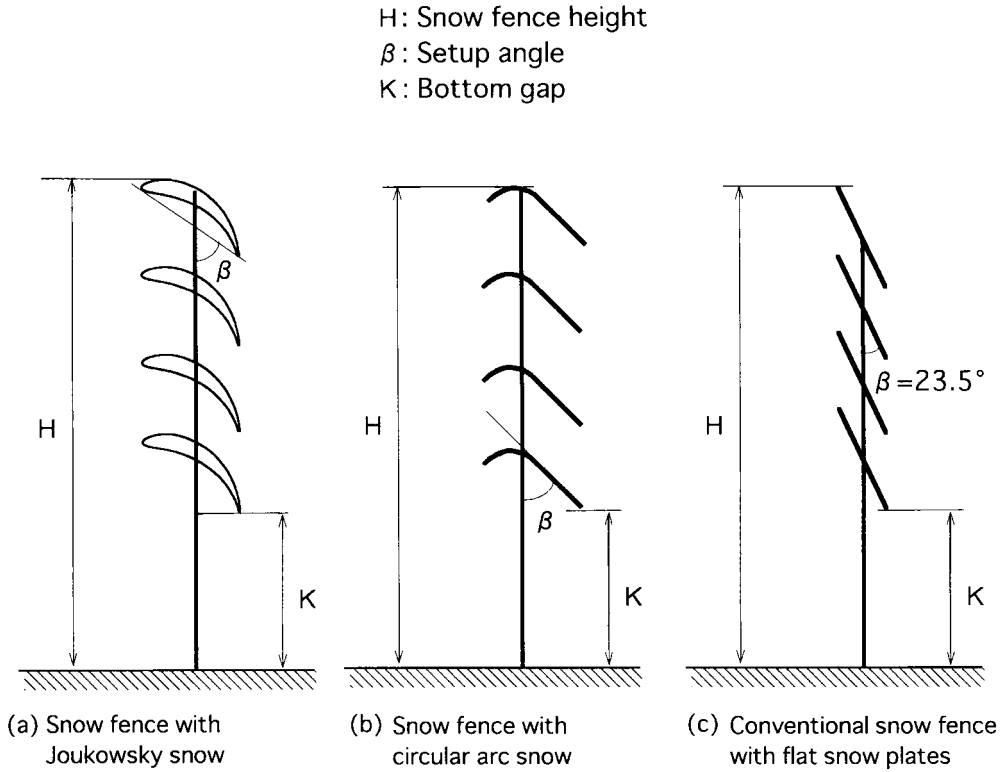
H: Snow fence height
β: Setup angle
K: Bottom gap

(a) Snow fence with
Joukowsky snow

(b) Snow fence with
circular arc snow

(c) Conventional snow fence
with flat snow plates

Fig. 4   Snow fence configurations

3. SIMILARITY LAW OF BLOWING-SNOW SIMULA-TION IN A WIND TUNNEL USING SNOW PARTICLES

Six parameters govern the flow of blowing snow around a snow fence: the approaching velocity, U; the height of the snow fence, H; the diameter of the snow particle, d; the gravity, g; and the viscosity, μ, and density of the fluid, ρ. When the three repeat variables U, H, and ρ are adopted, three non-dimensional parameters are produced based on the Buckingham Π theorem:

(1)   The Reynolds number based on the height of the snow fence, R_H ($=UH/\nu$)

(2)   The Froude number based on the height of the snow fence, F_H ($=U/\sqrt{gH}$)

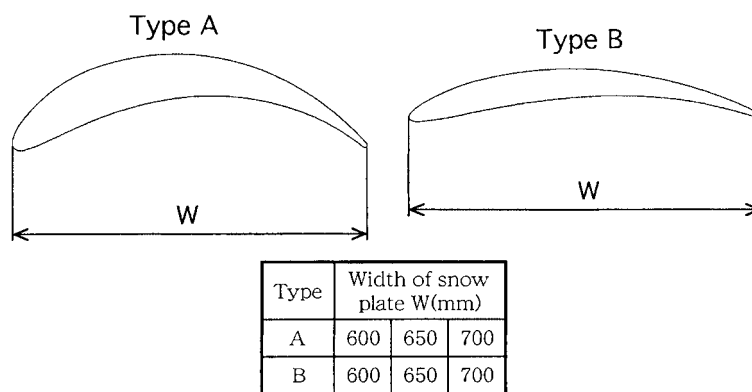(3)   The ratio between the diameter of the snow particles and height of the snow fence, d/H

Moreover, by adopting the three repeat variables U, d, and ρ, three non-dimensional parameters are produced:

(1)   The Reynolds number based on the diameter of the snow particles, R_d ($=Ud/\nu$)

(2)   The Froude number based on the diameter of the snow particles, F_d ($=U/\sqrt{gd}$)

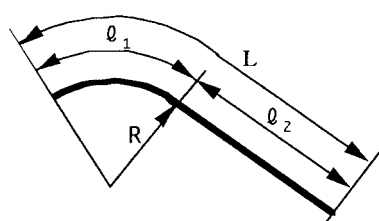(3)   The ratio between the diameter of the snow particles and height of the snow fence, d/H

First, consider the Reynolds numbers R_H and R_d. Rd does not need to be taken into account because it becomes identity between the real and the model case when natural snow particles are used as the snow model. Moreover, there is hardly any effect of the Reynolds number on flow together with separation, such as occurs around the snow fence when the Reynolds number exceeds 10^4. The R_H of our snow fence model is $(1.68-3.0)\times10^5$, and the R_H of the prototype snow fence 1.8×10^6. Consequently, it is not necessary to consider the Reynolds number R_H, because for the model and prototype snow fence it exceeds 10^4. On the basis of the dimensionless parameter d/H, a snow particle size of $1/n$ must be adopted when the dimension of the snow fence model is $1/n$ the scale of the prototype. Because snow particle motion is greatly dependent on R_d at a low Reynolds number (R_d based on a snow particle diameter of d =0.1 mm−0.2 mm is 50−100), snow particle motion in the test model differs considerably from the actuality when the size of the snow particle model is $1/n$. A method in which R_d is made to agree with the dimensionless parameters of R_d and d/H therefore should be adopted.

Next, consider the Froude numbers F_H and F_d. In nature, snow particles usually begin to blow at a wind velocity of U=6 m−7 m/s. If the Froude number, F_H, based on the height H of the snow fence governs the similarity law, the snow particles in the test model begin to blow at U=1.9 m/s−2.2 m/s when scale of the snow fence model is 1/10 that of the prototype. The wind velocity at which the snow particles blow in the wind tunnel using snow particles is U=6 m/s−7 m/s, as in nature. As a result, F_H can not be a parameter that governs the similarity law. F_d, which is based on the diameter d of the snow particle therefore governs the similarity law. Consequently, the parameters that govern the flow of blowing snow around a snow fence are the Reynolds number, R_d, and the Froude number, F_d. In our experiment, R_d and F_d both in the test model and in reality are identical because actual snow particles were used in the particle model. Results obtained with the test model therefore can be regarded as reproducing the actual result for an equivalent wind velocity. Figure 6 gives a comparison of snowdrift shape for the wind tunnel test model and a field

DEVELOPMENT OF A NEW TYPE SNOW FENCE WITH AIRFOIL SNOW PLATES TO PREVENT BLOWING-SNOW DISASTERS:
PART 1, EVALUATION OF PERFORMANCE BY BLOWING-SNOW SIMULATION IN A WIND TUNNEL

5

Type A   Type B

Type	Width of snow plate W(mm)		
A	600	650	700
B	600	650	700

(a) Joukowsky airfoil snow plate

Type	Length of snow plate L(mm)	Length of circular arc ℓ_1(mm)	Length of flat plate ℓ_2(mm)	Radius of circular arc R(mm)
A	520	300	220	223
	620	357	263	266
	950	547	403	408
B	520	270	250	264
	620	322	298	315
	950	493	457	483

(b) Circular arc airfoil snow plate

Fig. 5   Airfoil snow plate configuration

observation experiment made with the prototype snow fence. Because these snowdrift shapes are very similar, the wind tunnel test model that uses actual snow particles reproduces the results for reality in proportion to wind velocity with considerable accuracy.

4.   RESULTS AND DISCUSSIONS

4.1   Method of evaluating snow fence performance

In the blowing-off type snow fence, blowing snow which passes through the snow plates and the bottom gap must be transferred along the road surface without forming snowdrifts. To improve the blowing-off performance, any decrease in flow velocity along the roads surface and any rolling-up must be suppressed as much as possible. Snow fence performance can therefore be evaluated by two methods: One is to examine the characteristics of flow behind the snow fence, particularly bottom gap flow. The other is to examine the density of the blowing snow behind the fence (Haniu et al. 1995). We used these two methods to evaluate the performance of the snow fence.

4.2   Parameters governing snow fence performance

Six parameters govern the performance of the snow fence: (1) snow plate shape, (2) snow plate size W, (3) snow plate setup angle β, (4) number of snow plates n, (5) height of the bottom gap K, and (6) snow fence height H. In our study, the number of the snow plates was limited to n=4 because the standard snow fence is composed of four snow plates. In addition, the height of the snow fence, H, was kept constant at 2.8 m because standard snow fence height usually is approximately 3 m. The remaining four parameters were examined in detail to evaluate the performance of our newly developed snow fence.

4.3   Performance evaluation based on blowing-snow density

4.3.1   Airfoil snow plate shape

Figure 7 shows spatial density distributions of blowing snow around a snow fence constructed different snow plate shapes. Two types of Joukowsky airfoil snow plates and circular arc airfoil snow plates were used (Fig.5). Density distributions of the blowing snow were measured by the image-processing method. This

method is based on the fact that the strength of scattered light from a slit light source changes with the spatial concentration of snow particles. A computer was used to divide the recorded images into an intensity distribution of 256 grades, and blowing-snow density was evaluated by classifying the grades in the six ranges shown in Table 1. As the gradation number increases, the blowing snow gradually reaches a high density. Snow fence performance based on the density distribution of blowing snow also can be evaluated as follows: (1) blowing snow passes over a region lower than the driver's eye level of 1.35 m, (2) blowing snow passes as near the road surface as possible.

First, consider a snow fence constructed with Joukowsky airfoil snow plates: More blowing snow of high density passes in the vicinity of the road surface with Type A which has a large camber line than with Type B which has a small one. This seems to be caused by a difference in the deflection of blowing snow that passes through the snow plates toward the road due to the difference in the camber lines. The blowing-off performance of a snow fence
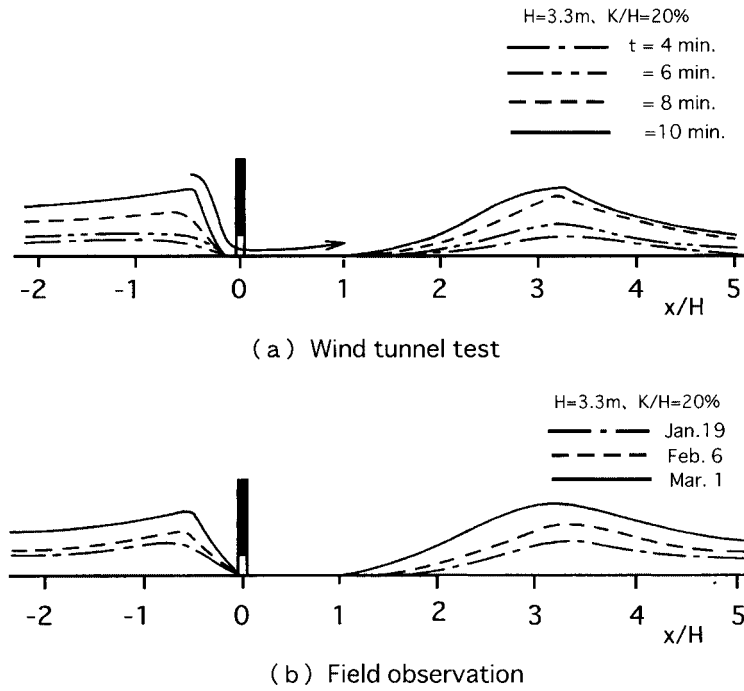

(a) Wind tunnel test

(b) Field observation

Fig. 6   Comparison of snowdrifts formed with the wind tunnel model and full-scale fence

(a) Snow fence with Joukowsky airfoil snow plate

(b) Snow fence with circular arc airfoil snow plate

(c) Conventional snow fence
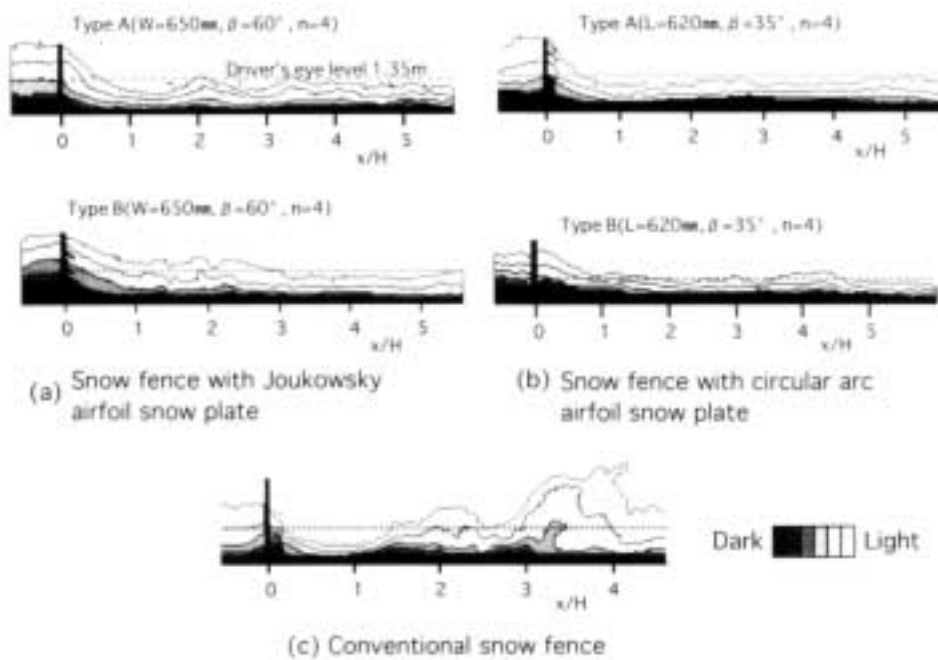
Fig. 7   Density distributions of blowing snow for different snow plates shapes

DEVELOPMENT OF A NEW TYPE SNOW FENCE WITH AIRFOIL SNOW PLATES TO PREVENT BLOWING-SNOW DISASTERS:
PART 1, EVALUATION OF PERFORMANCE BY BLOWING-SNOW SIMULATION IN A WIND TUNNEL

7

with Type A snow plates therefore is higher than that of one with Type B snow plates. Now consider a snow fence with circular arc airfoil snow plates. The blowing-off performance of Type A snow plate is slightly better than that of Type B snow plates which have a smaller circular arc. For comparison, the blowing-snow density distribution around a conventional snow fence with the flat snow plates is shown in Fig.7(c). The rolling-up of blowing snow occurs from the position $x/H=1.5-2.0$ behind the snow fence, then high density, blowing snow passes over the spatial region higher than the driver's eye level (1.35 m). The performance of a snow fence with airfoil snow plates is markedly improved in comparison to that of a conventional snow fence. Most high density blowing snow that passes the snow fence with the airfoil snow plates moves along the roads surface with no rolling-up, even at distances from

the fence that exceed $x/H=5.0$. A snow fence with the airfoil snow plates therefore would be sufficient for a wide road with a width exceeding 20 m.

4.3.2　Snow plate size

Figure 8 shows the spatial density distribution of blowing snow around snow fences that have the snow plates of various sizes. Figure 8(a) shows results when the size of Joukowsky airfoil snow plate (Type A) is W=600, 650, and 700 mm, and Figure 8(b) when the size of the circular arc airfoil snow plate (Type A) is L=520, 620, and 950 mm. The snow fence height and the bottom gap are constant at H=2.8 m and K=1.2 m. The setup angles are β =60° for the Joukowsky airfoil snow plate and β =35° for the circular arc airfoil snow plate. In the case of a snow fence with Joukowsky airfoil snow plates, performance improves as the
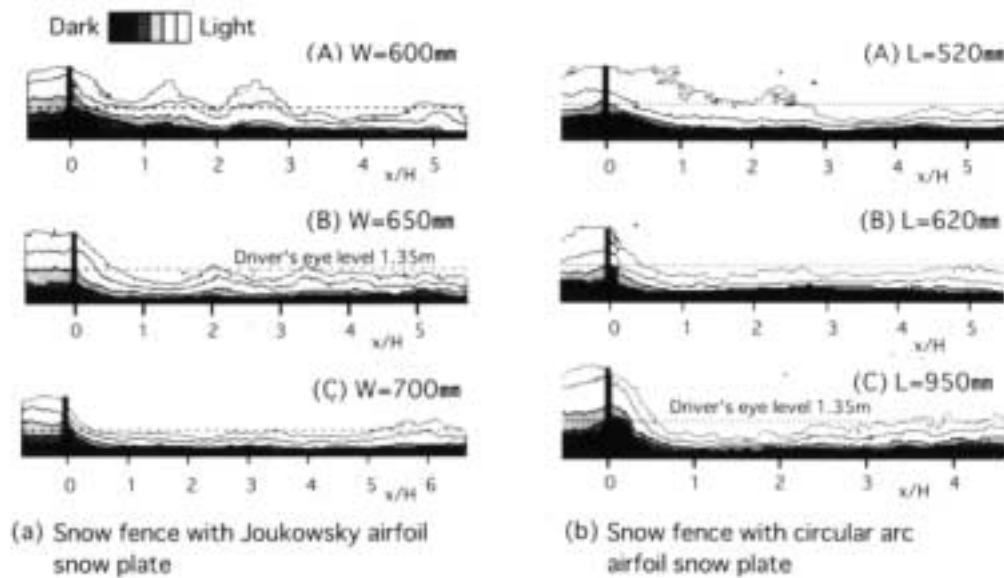

Fig. 8　Density distributions of blowing snow for different snow plate sizes
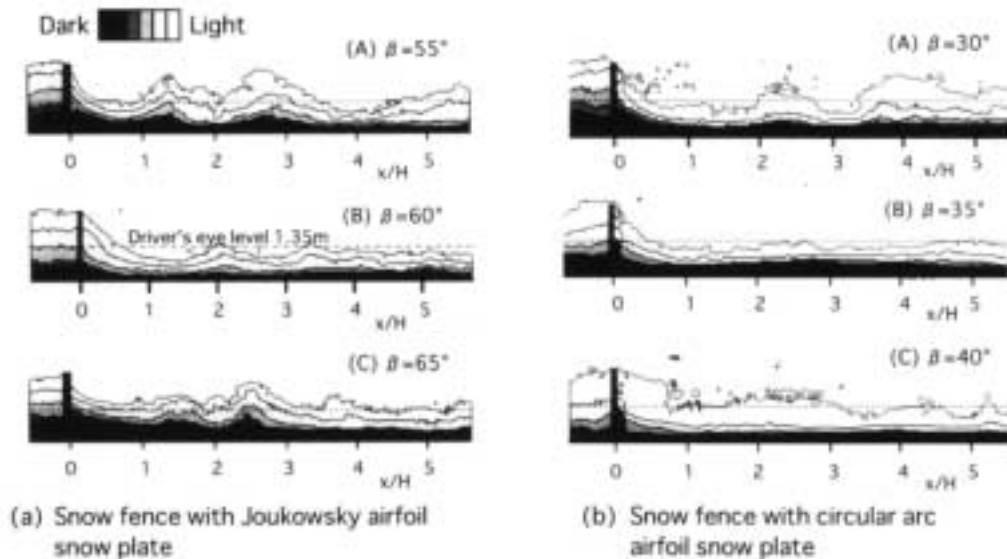

Fig. 9　Density distributions of blowing snow for different snow plate setup angles β

width, W, increase, and similarly for a snow fence with circular arc airfoil snow plates. In contrast, for a Joukowsky airfoil snow plate of W=600 mm and a circular arc airfoil snow plate of L=520 mm, blowing snow passes in the spatial region beyond the driver's eye
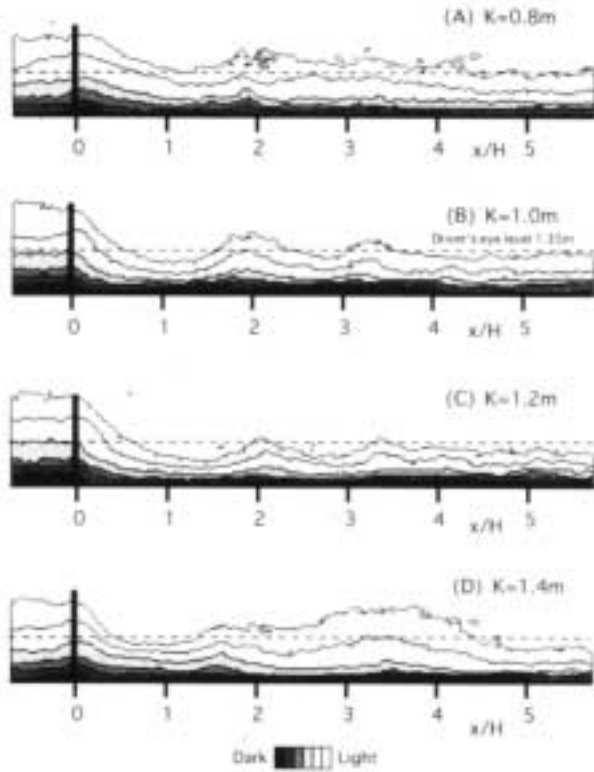

Fig. 10   Density distributions of blowing snow for different bottom gaps

level (1.35 m), and the snow fence performance decreases. A Joukowsky airfoil snow plate of W=650 mm and a circular arc airfoil snow plate of L=620 mm therefore are judged to be the minimum acceptable sizes.

4.3.3   Snow plate setup angles

Figure 9 shows the density distributions of blowing snow for various setup angles, β, of the snow plate. The height of the snow fence is constant at H=2.8 m. For Joukowsky airfoil snow plate (Type A), shown in Fig.9(a), the selected height of the bottom gap is K=1.2 m, and the selected snow plate size W=650 mm. For the circular arc airfoil snow plate (Type A), K=1.2 m and L=620 mm are the values. With a snow fence that has Joukowsky airfoil snow plates, because the vortex region formed behind the snow fence is large at the setup angle of β=55°, the flow passing through the bottom gap is rolled up lowering the blowing-off performance. Moreover, at β=65°, because there is little deflection of the blowing snow passing through the snow plates, the blowing-off performance also is lowered. The optimum value of the setup angle, β, therefore is approximately 60°. As is clear from Fig.9(b), the optimum value of the setup angle is approximately β=35° for a snow fence with the circular arc airfoil snow plates.

4.3.4   Height of the bottom gap

Figure 10 shows the density distributions of blowing snow around a snow fence with Joukowsky airfoil snow plates for different bottom gap heights. The fence had a height of H=2.8 m, snow plate size of W=650 mm, and setup angle of β=60°. For K=0.8 m and 1.0 m, because the interval between snow plates installed at regular intervals is large, blowing snow that passes through the plates traverses the road at a level higher than the driver's eye (1.35 m). For K=1.2 m, most of the blowing snow that passes through the snow plates traverses the spatial region lower than the driver's eye level. For K=1.4 m, rolling-up of the blowing snow
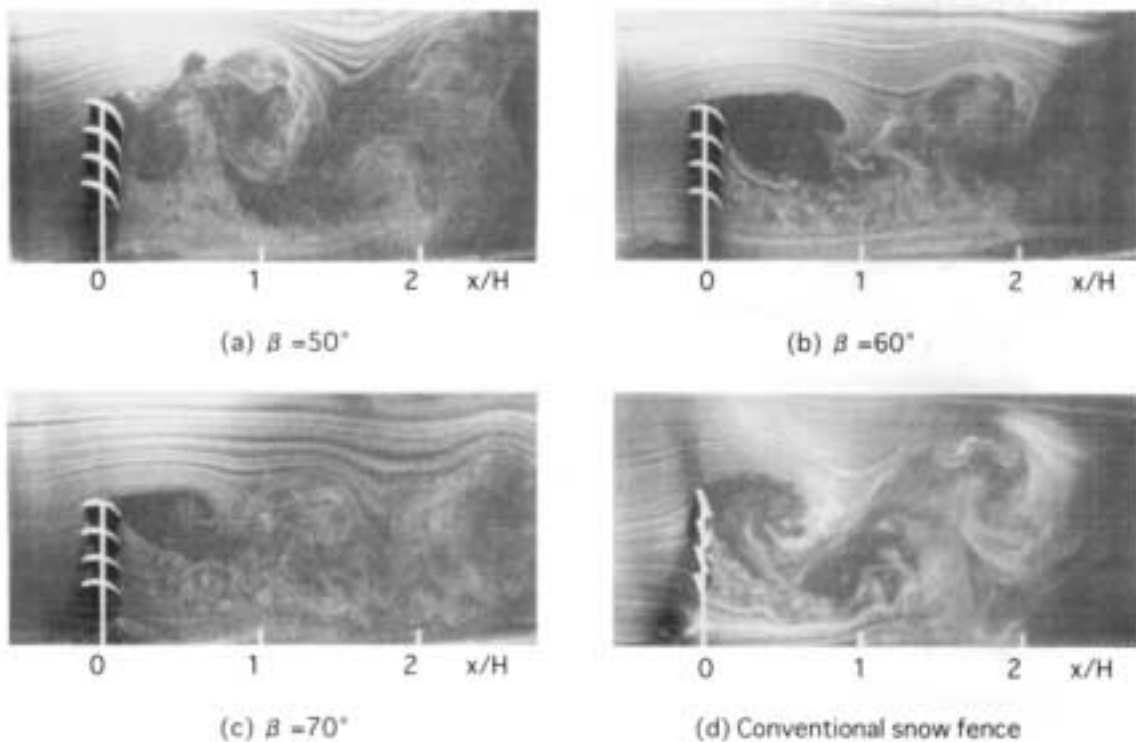

Fig. 11   Visualization of flow patterns around snow fence

*DEVELOPMENT OF A NEW TYPE SNOW FENCE WITH AIRFOIL SNOW PLATES TO PREVENT BLOWING-SNOW DISASTERS:
PART 1, EVALUATION OF PERFORMANCE BY BLOWING-SNOW SIMULATION IN A WIND TUNNEL*

9

behind the snow fence occurs, producing a lower blowing-off performance for the snow fence. Optimum height of the bottom gap, *K*, therefore is approximately 1.2 m when snow fence height is *H*=2.8 m. Moreover, the optimum height of the bottom gap, *K*, is approximately 1.2 m for a snow fence with circular arc airfoil snow plates.

4.4 Performance evaluation based on the flow pattern

The performance of a snow fence can be evaluated by observing the flow pattern. The flow pattern around a snow fence with Joukowsky airfoil snow plates was determined. The snow fence height was *H*=2.8 m, bottom gap height *K*=1.2 m, and snow plate size *W*=650 mm. Figure 11 shows the flow patterns around a snow fence when the setup angle, β, of the snow plates is changed. At β=50°, the flow which passes over the topmost part of the snow fence and that which passes through the bottom gap roll up alternately behind the snow fence, causing a large-scale vortex. This phenomenon leads to high-density blowing snow being spread over the entire area behind the snow fence. At β=60°, the flow passes through the snow plates is deflected toward the roads surface, then moves along that surface together with the bottom gap flow, but with no rolling-up of the flow downstream. This flow pattern produces a large blowing-off effect. At β=70°, there is no rolling-up of the flow behind the snow fence. Because deflection of the flow that passes through the snow plates is small, a considerable amount of blowing snow with high-density passes over the fence in the high spatial region such that visibility blockage may occur. The flow pattern around a conventional snow fence is shown in Fig.11 (d). The flow approaching the snow fence is divided into top and bottom gap flows, which alternately roll up behind the snow fence. Due to the rolling-up of the bottom gap flow, snowdrifts and visibility blockage occur at the position *x*/*H*=1.5~2.0. To improve the blowing-off performance of the snow fence, the vortex region formed behind the fence should be decreased as much as possible, thereby preventing the rolling-up of the bottom gap flow.

4.5 Performance evaluation based on flow characteristics

4.5.1 Time-averaged velocity distributions

The time-averaged velocity distributions behind the snow fence were measured to evaluate the characteristics of bottom gap flow and the vortex region formed behind the fence, both of which govern snow fence performance. For the time averaged-velocity distribution measurements, a snow fence with Joukowsky airfoil snow plates, whose blowing-off performance was highest in the blowing-snow simulation test, was used. Specifically, this snow fence had a height of *H*=2.8 m and bottom gap height of *K*=1.2 m. The size of its snow plates was *W*=650 mm and the setup angle β =60°. The time-averaged velocity distributions for a conventional snow fence also were measured for comparison. Figure 12 shows the equi-velocity lines for the velocity *u* in the *x* flow direction. For the conventional snow fence, bottom gap flow accelerates considerably after passage through the snow fence, whereas bottom gap flow along the road surface decelerates quickly and flows upward from the approximate position of *x*/*H*=2.0. High-density blowing snow that passes through the bottom gap therefore gets rolled up due to its upward flow, lowering the blowing-off performance of the snow fence. A acceleration of bottom gap flow is low with the newly developed snow fence. Moreover, deceleration of the bottom gap flow at downstream is small, and the bottom gap flow moves along the road surface without rolling-up, therefore, the newly developed snow fence produces a high blowing-off .

Consider the vortex region formed behind the snow fence. For a conventional snow fence it is a large-scale vortex that covers the entire snow fence. With the newly developed snow fence, the vortex region forms only at the rear of the snow plate at the topmost part of the snow fence. This reduction in the vortex region of the snow fence with the airfoil snow plate produces so little rolling-up of the bottom gap flow that blowing-off performance is markedly improved as compared to that of the conventional snow fence.

4.5.2 Momentum of bottom gap flow

Momentum along the road surface governs the transportation of blowing snow. Figure 13 shows the momentum of bottom gap flow calculated from the time-averaged velocity distributions. Here, the *M*/*M₀* of the ordinate axis is the momentum calculated by equation (1), and the abscissa axis is the distance, *x*/*H*, from the snow fence.

$$M=\int_0^k \rho Q \mathrm{v}\cos\theta = \int_0^k \rho (\mathrm{v}\cos\theta)^2 dy$$

$$(1)$$

$$M_0=\int_0^k \rho \, kU^2$$

(a) Snow fence with Joukowsky airfoil snow plate
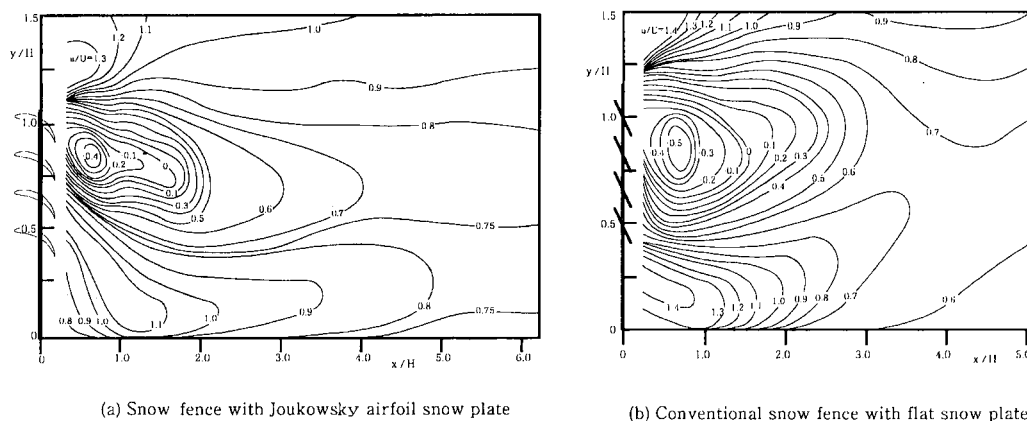
(b) Conventional snow fence with flat snow plate

Fig. 12 Equi-velocity line behind snow fence models

Here, v is the absolute velocity, θ the angle between the direction of absolute velocity and the x-axis, U the approaching flow velocity, and K the height of the bottom gap. M_0 is the momentum when the flow velocity passing through the bottom gap is the approaching velocity U. For the conventional snow fence, the momentum of the bottom gap flow immediately after passage through the snow fence is considerably large, whereas the decrease in momentum is large in the downstream, approximately 25% of the momentum immediately after passage through the snow fence at x/H=5.0. For the newly developed snow fence, the momentum immediately after passage through the snow fence is less than that of the conventional snow fence, but the decrease in momentum in the downstream direction is small, significant momentum being retained; 75% of the momentum immediately after passage through the snow fence at x/H=5.0. The increase in momentum at approximately x/H=1.7 is due to the addition of the momentum of the flow that passes through the snow plate. The blowing-off performance of the newly developed snow fence therefore is improved because the decrease in momentum in the downstream is considerably less than that for the conventional snow fence.

4.6 Performance evaluated by a field observation experiment

A snow fence model with the circular arc airfoil snow plates of L=950 mm was used in the field observations. This model, overall length of 30.4 m, was installed contiguous to a conventional snow fence to allow comparison. For snowdrift evaluation, three poles were installed windward of the snow fence and ten poles leeward in the direction of the road.

Figure 14 shows the snowdrift formation findings from December 27, 1997 to February 6, 1998. There was no blockage of the bottom gap generated by snowdrifts upstream of the newly developed snow fence, whereas there was for the conventional snow fence, because the snowdrift volume was extremely large. Blowing-off performance is always retained with the newly developed snow fence because there is no blockage of the bottom gap by snowdrifts. Leeward of the road, the maximum snowdrift height is approximately 50 cm for the newly developed snow fence, whereas for the conventional one it is approximately 200 cm. With the newly developed snow fence, there are almost no snowdrifts for a distance of 30 m on the leeward side. The newly developed snow fence therefore appears to retain the blowing-off effect over a considerable distance.
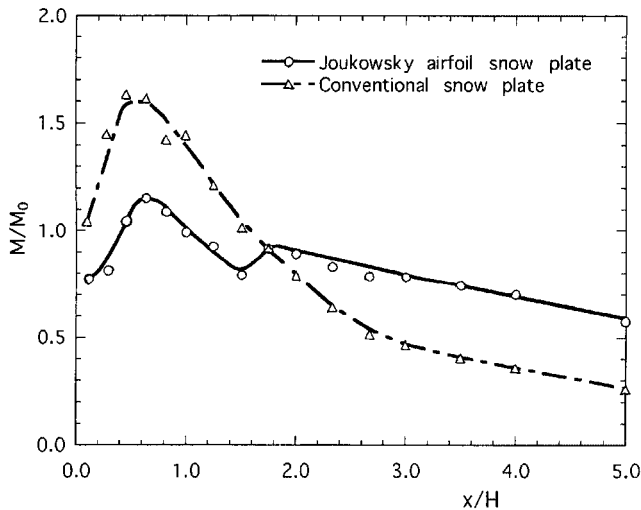

Fig. 13   Momentum of bottom gap flow of snow fences

2. CONCLUSIONS

(1)   In the wind tunnel experiment made with actual snow particles, the similarity law is prescribed by the Froude number, F_d, based on the diameter, d, of the snow particles

(2)   The vortex region formed behind the snow fence induces rolling-up of bottom gap flow. This vortex region therefore must be reduced as much as possible to improve the blowing-off performance of the snow fence.

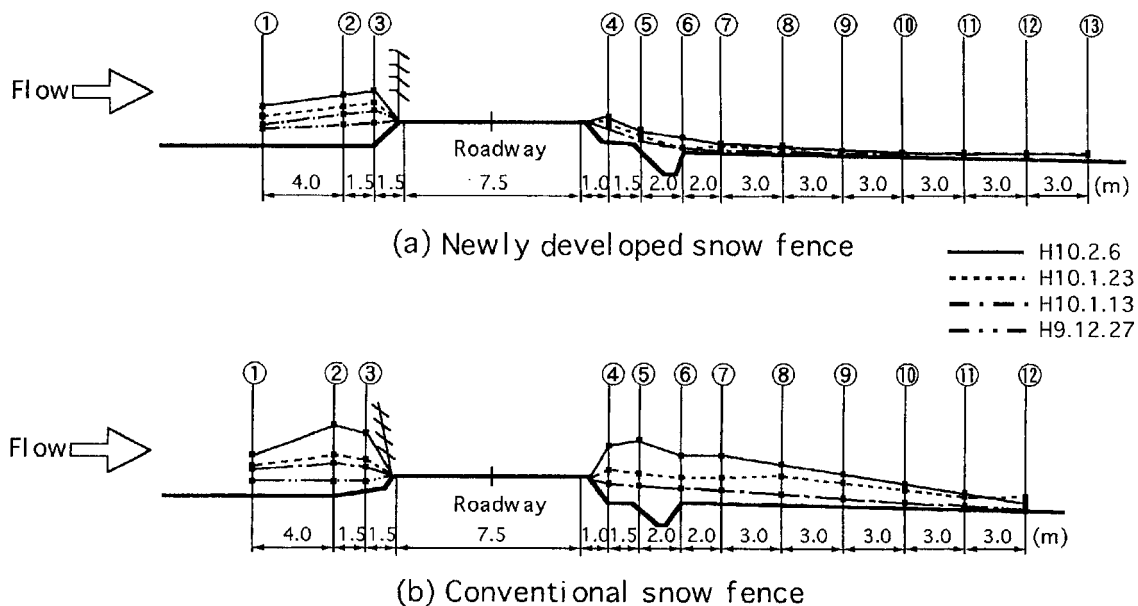(3)   The vortex region formed behind the snow fence with the air-

Fig. 14   Field observations of a full-scale snow fence model for snowdrifts

DEVELOPMENT OF A NEW TYPE SNOW FENCE WITH AIRFOIL SNOW PLATES TO PREVENT BLOWING-SNOW DISASTERS:
PART 1, EVALUATION OF PERFORMANCE BY BLOWING-SNOW SIMULATION IN A WIND TUNNEL

11

foil snow plates is considerably reduced, such that rolling-up of bottom gap flow completely is suppressed.

(4) The size and setup angle of the airfoil snow plate and height of the bottom gap are the parameters that govern snow fence performance. We determined the optimum size and setup angle of the snow plate and the height of the bottom gap.

(5) Both the wind tunnel and field observation experiments showed that the blowing-off performance of the snow fence with airfoil snow plates is markedly improved as compared to that of the conventional snow fence.

ACKNOWLEDGMENTS

REFERENCES

Ishimono, K., Takeuchi, M., Nohara, T. and Fukuzawa, Y., 1984. A study on snow fences, Ice and Roads, 1, 96-100. (in Japanese).

Haniu, H. and Sakamoto, H., 1995. Improvement of blower type snow fences by control of the shear layer, Journal of Natural Disaster Science, 17-1, 53-64.

Sakamoto, H., Haniu, H, Kiyota, M. and Obata, Y., 1992. Development and performance of snow fences for prevention of blowing-snow disasters, Transactions of the Japan Society of Mechanical Engineers (B), 58-550, 2017-2023. (in Japanese).

Sakamoto, H., 1999. Estimation of snow-fence performance by a wind tunnel simulation test, Bulletin of the Natural Disaster Science Data Center Hokkaido, 13, 53-65. (in Japanese).

Takeuchi, M., 1989. Snow-collection mechanism and the capacities of snow fences, Annuals of Glaciology, 13, 248-251.

Takeuchi, M., 1996. For the control of blowing snow, Journal of the Japanese Society of Snow and Ice, 58-2, 161-168. (in Japanese).

Yamada, T., Akitaya, A. and Tachibana, Y., 1988. Disasters created by snow and ice in Hokkaido, Proceedings of the '88 Cold Region Technology Conference, 179-184. (in Japanese).

NOMENCLATURE

F_d : Froude number based on snow particle diameter

H : height of the snow fence

K : height of the bottom gap

L : size of the circular arc airfoil snow plate

M : momentum of the bottom gap flow

M_0 : momentum of the bottom gap flow based on velocity U

R_H : Reynolds number based on snow fence height

U : approaching flow velocity

u : velocity in the x direction

v : absolute velocity

W : size of the Joukowsky airfoil snow plate

x , y : cartesian coordinate system

β : setup angle of the snow plate

θ : angle between the direction of absolute velocity and x-axis

ν : kinematic viscosity of fluid

ρ : density of fluid

μ : viscosity of fluid.